SOME MEASUREMENTS OF PHASE VELOCITY ALONG A HELIX WITH DIELECTRIC SUPPORTS

L. A. HARRIS
H. R. JOHNSON
A. KARP
L. D. SMULLIN

TECHNICAL REPORT NO. 93

JANUARY 21, 1949

RESEARCH LABORATORY OF ELECTRONICS
MASSACHUSETTS INSTITUTE OF TECHNOLOGY

The research reported in this document was made possible through support extended the Massachusetts Institute of Technology, Research Laboratory of Electronics, jointly by the Army Signal Corps, the Navy Department (Office of Naval Research) and the Air Force (Air Materiel Command), under Signal Corps Contract No. W36-039-sc-32037, Project No. 102B; Department of the Army Project No. 3-99-10-022.

MASSACHUSETTS INSTITUTE OF TECHNOLOGY

Research Laboratory of Electronics

Technical Report No. 93 January 21, 1949

SOME MEASUREMENTS OF PHASE VELOCITY ALONG A HELIX WITH DIELECTRIC SUPPORTS

L. A. Harris

H. R. Johnson

A. Karp

L. D. Smullin

Abstract

Measurements of the propagation characteristics of several helices are described. The tendency of some traveling-wave tubes to oscillate at about half their nominal operating frequencies is explained in terms of the gain and phase-velocity characteristics as functions of frequency.

The external dielectric supporting structures generally decrease the dispersion of the helix, and may even cause a minimum to appear in the velocity-frequency characteristic. Tubular helix supports and dielectric-rod supports are examined, and a new type of low-dielectric-constant support is suggested.

The effect of finite wire diameter is to restore some of the helix dispersion. Thus, an actual helix in a thick dielectric tube is more dispersive than the equivalent thin helical sheath in a similar tube.

SOME MEASUREMENTS OF PHASE VELOCITY ALONG A HELIX WITH DIELECTRIC SUPPORTS

Introduction

The traveling-wave amplifier tubes described by Kompfner (1) and Pierce (2) convert the d-c kinetic energy of electrons in a beam into high-frequency energy by causing the electrons and the radio-frequency wave to travel at almost synchronous velocities for a time which is large compared to the period of the r-f wave. In this way, the usual transit-time difficulties encountered in more conventional tubes are overcome.

For practical reasons, it is desirable to keep the accelerating voltages on an amplifier tube below a few thousand volts. The resulting electron velocities are of the order of 0.1c ($\sim 3 \times 10^9$ cm/sec). Thus the wave must be made to travel more slowly than the velocity of light. Several different types of waveguides which will propagate such slow waves are known. The one that has proved most useful is the helix. It combines good coupling to the electron beam with very low dispersion, and it is relatively easy to build.

The work reported here was undertaken to determine wherein the physical helix differed from the idealized current-sheath model used for most analyses of the helix (2),(3),(4). Mechanically, the physical helix differs from the idealized current sheath in two important respects: (a) the diameter of the wire may be as much as 10 to 20 per cent of the helix diameter, and 50 per cent of the distance between wires; and (b) the helix is usually supported by some external dielectric structure which is uniform along the axis, but is not uniform either radially or circumferentially.

The direct incentive for undertaking these studies was the desire to understand and eliminate the tendency of many traveling-wave tubes to oscillate. The oscillations have been observed to occur at roughly one-half to one-third of the nominal operating frequency of the tubes and at beam voltages which give optimum gain in the design band.

A necessary condition for the occurrence of self-sustained oscillations is

$$\left| G \, \Gamma_1 \, L \, \Gamma_2 \right| = 1$$

where G is the forward gain, Γ_1 is the reflection coefficient at the output end of the helix, L is the attenuation of the reflected wave and Γ_2 is the reflection coefficient at the input end. Within the pass band, $\left| \Gamma_1 \, \Gamma_2 \right| < 1$, while outside this band $\left| \Gamma_1 \, \Gamma_2 \right| \simeq 1$.

The oscillations were observed at the voltage giving maximum gain

in the pass band, but at currents small enough so that the product $|G\ L| \ll 1$ in the pass band. There appear to be two independent phenomena responsible for this behavior. One of these is the dependence of gain on the helix diameter, the other is the shape of the phase velocity-frequency characteristic of the actual helix (as distinct from the mathematical model).

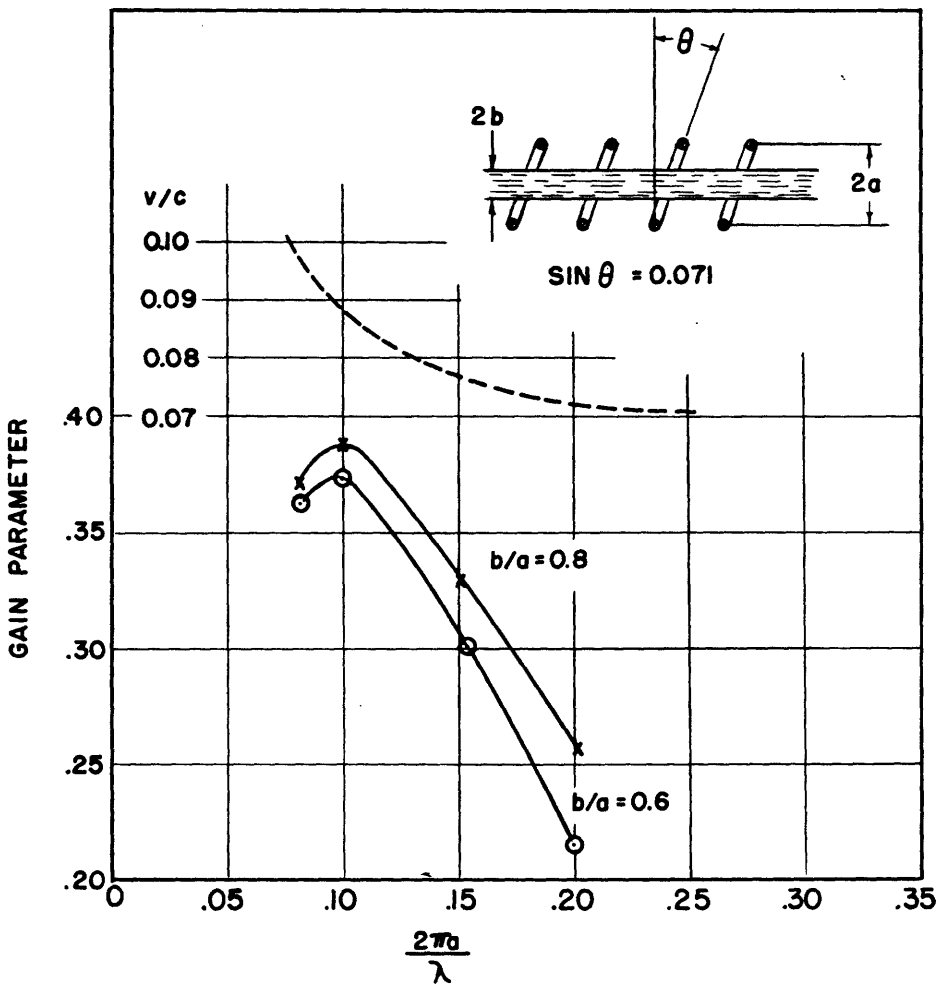

Fig.1 Computed gain and velocity characteristics of traveling-wave tube with unsupported helix, plotted as functions of frequency.

Figure 1 shows the computed gain constant of the amplified wave as a function of frequency for a given helix, and for two different beam diameters. It is assumed that the beam voltage is adjusted for maximum gain at each frequency. The theoretical phase-velocity curve for this helix is also shown. The curves are computed from the formulae in Rydbeck's paper (4).

Many of the tubes built in various laboratories in the past few years had helices such that $2\pi a/\lambda \approx 0.2$ in the pass band (a = helix radius). According to Figure 1, the gain is considerably greater at $2\pi a/\lambda \approx 0.1$, or at about one-half the design frequency of these tubes; moreover, the re-

sistive losses in the helix will be less at the lower frequency. Thus we see that $|GL|$ may be much greater at the oscillation frequency than it is in the pass band. The oscillations, however, were observed to occur when the electron velocity was equal to the phase velocity in the pass band. According to Figure 1 the velocity at the lower frequencies is 10 to 20 per cent greater. Analysis indicates that gain is obtained only when the electron velocity is within about 1 per cent of the wave velocity (3),(4). Thus, although it is clear that conditions for oscillations may be satisfied at about half the design frequency, the simple theory indicates that they will be satisfied only at beam voltages considerably above the design voltage. The results of the experiments to be described help to resolve this anomaly.

Experimental Results

The measurements were made in two different frequency regimes. The first experiments were made at 9100 Mc/sec with the apparatus shown in Figure 2. A recording of the standing-wave pattern along the helix is shown in Figure 3. No direct analysis of this pattern was made; instead,

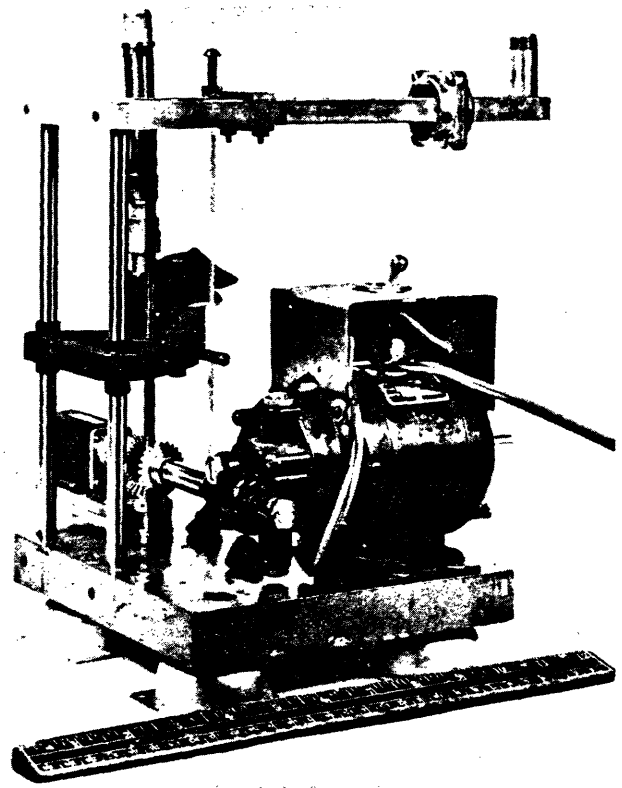

Fig.2 Apparatus for recording standing-wave pattern along helix at 9100 Mc.

a solution was assumed and checked against the observed pattern. Shulman and Heagy (5) predict the existence of modes with an angular dependence. In the usual range of operation of a helix, these higher modes have an axial velocity almost equal to that of light. It was assumed, therefore,

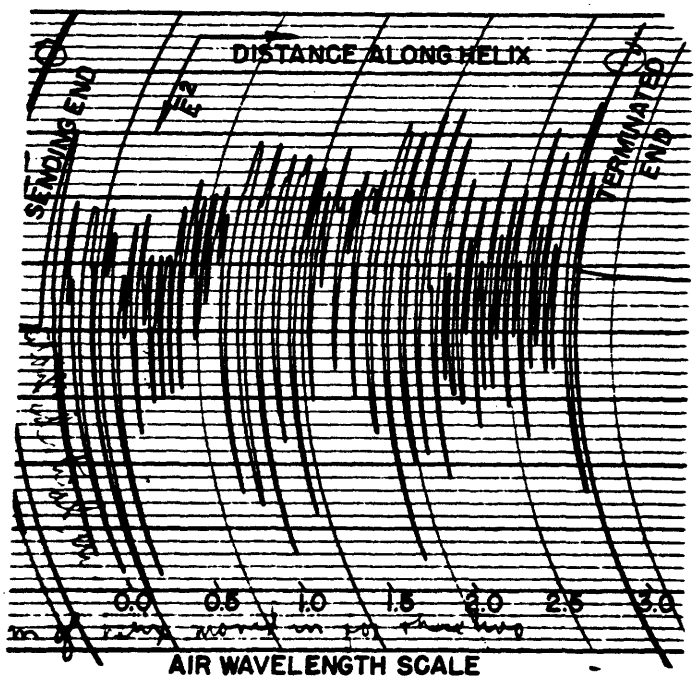

Fig.3 Recording of standing-wave pattern along helix at 9100 Mc.

that the standing-wave pattern was the result of a fast ($v \approx c$) mode and a slow ($v \approx 0.1\ c$) mode, each having a forward and a reflected wave. The periods of the various waves that would be measured by a square-law detector were computed and checked against the measured curve. The agreement was of the order of 4 per cent, which was deemed to be an adequate confirmation of the theory. No angular measurements were made, nor were these measurements pursued because of the experimental difficulties associated with the smallness of the apparatus.

The second group of measurements was made on large helices, scaled up by factors of 15, 30, from the 3-cm model, somewhat like the experiments of Cutler (6).

In the first arrangement, the helix was suspended by strings from a wooden frame. It was excited by simply attaching the inner conductor of a flexible coaxial line to the helix and stopping the outer conductor. Figure 4 is a plot of the distance between successive minima of the standing wave along the helix. This pattern has a definite beat character, and it can be shown that the presence of a fast and a slow wave produces such a pattern. In order to eliminate the fast mode, a tapered transition was used as shown in Figure 5. The flatter curve in Figure 4 shows the resulting improvement.

Figure 6 shows the measured phase velocity along this helix as a function of frequency. Curve A is for the "free-space" helix (suspended by strings). The agreement between theory and experiment is excellent if the mean diameter of the actual helix is used for computing the theoretical curve.

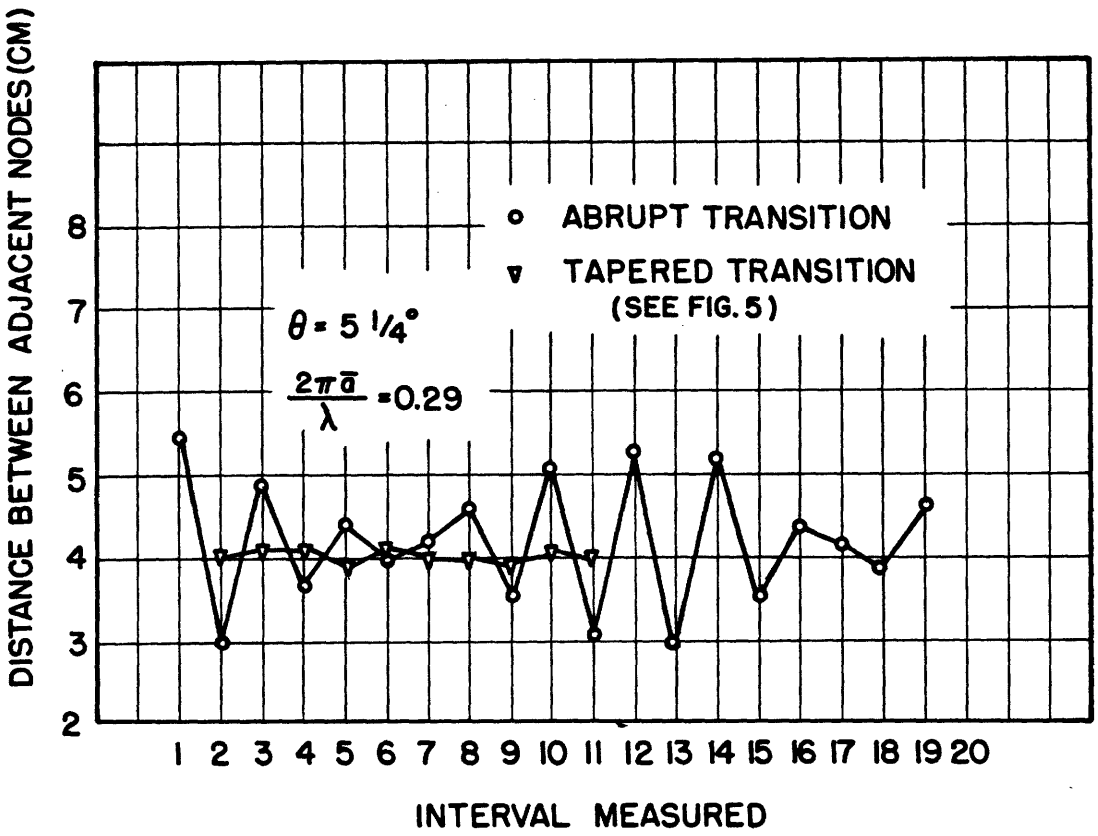

Fig.4 Variation of apparent half-wavelength in a probe measurement of standing waves along helix at 350 Mc, showing the effect of the method of transition.

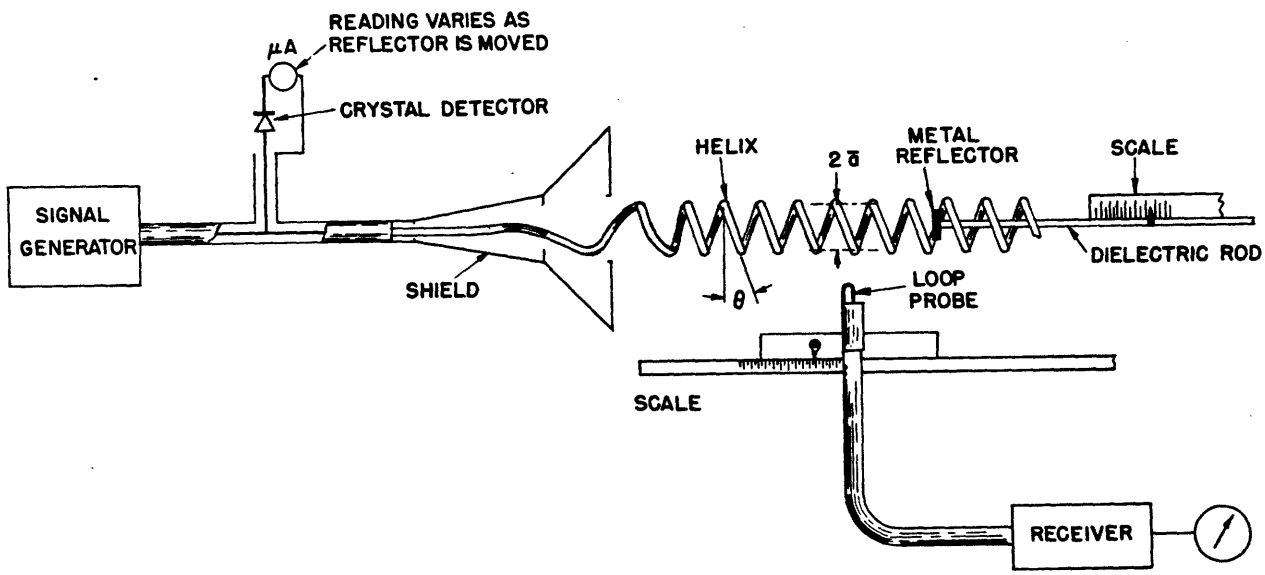

Fig.5 Apparatus used for velocity measurements on model helix. Helix and dielectric supports were suspended by strings.

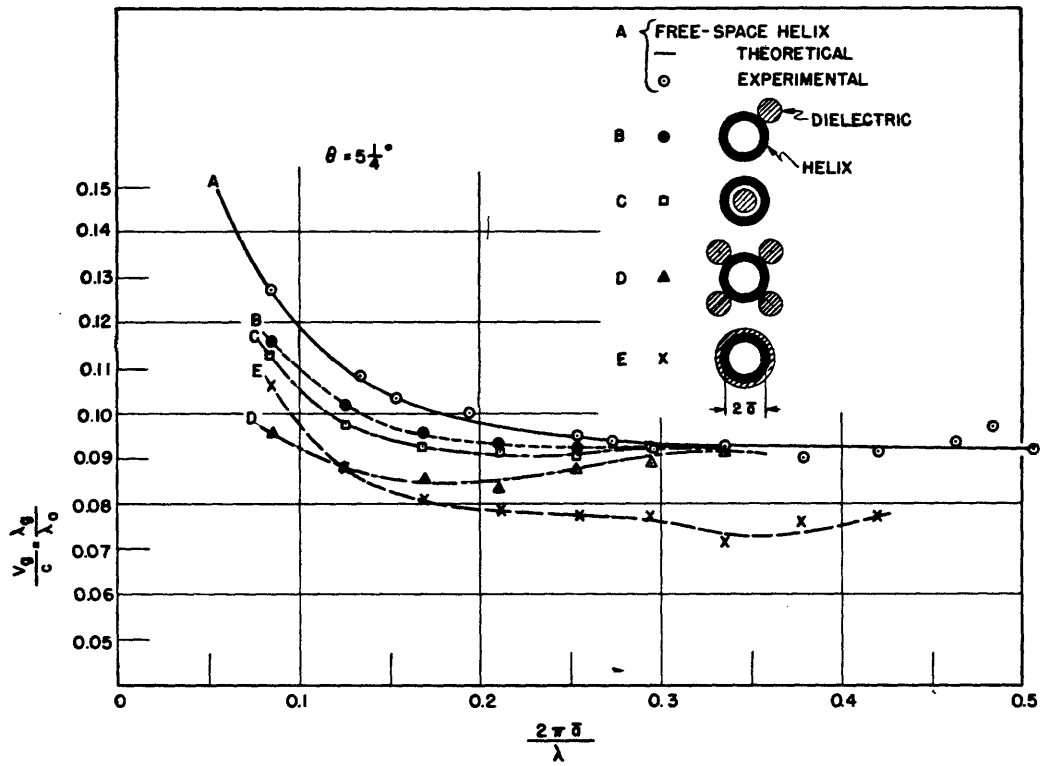

Fig.6 Measured phase-velocity characteristics of a charge-free helix supported by various dielectric structures.

Curves D and E represent the two most common methods of supporting the helix in a traveling-wave tube. The material used was bakelite with a dielectric constant of about 4.

Curve D, for the rod-supported helix, shows a marked dip in the velocity characteristic. In fact, the beam velocities required for gain are the same at $2\pi a/\lambda = 0.25$ and 0.12. This may well explain the observed low-frequency oscillations.

A qualitative explanation of this peculiar velocity characteristic may be found by considering the disposition of the dielectric about the helix. At high frequencies, the fields fall off so rapidly in the radial direction that only the part of the dielectric nearest the helix is effective in slowing the wave. At lower frequencies, the fields extend farther out, and the dielectric rods occupy a larger effective fraction of the space around the helix. At much lower frequencies, the fields extend out even farther, and the rods store an ever-decreasing fraction of the energy outside the helix. Hence, the velocity rises back toward that of the free-space helix at very long wavelengths.

Curve E represents the effect of a thin dielectric shell around the helix. The "normal" dispersive shape has been retained, but the velocity is reduced, as would be expected. This might represent a practical structure

for a 1000-Mc/sec tube, but not for higher-frequency tubes. The relative wall thickness of glass tubing increases rapidly with decreasing bore diameter, so that tubing suitable for supporting the helix of a 9000-Mc/sec tube would have a wall thickness comparable to the helix radius.

Figure 7 represents the results of some experiments on the effect of the thickness of a dielectric shell around an actual helix. Lengths of telescoping bakelite tubing were used to get the various thicknesses. Since there is no difference between the curves for the thickest and the next-thickest dielectric, we can assume they represent an infinitely thick dielectric.

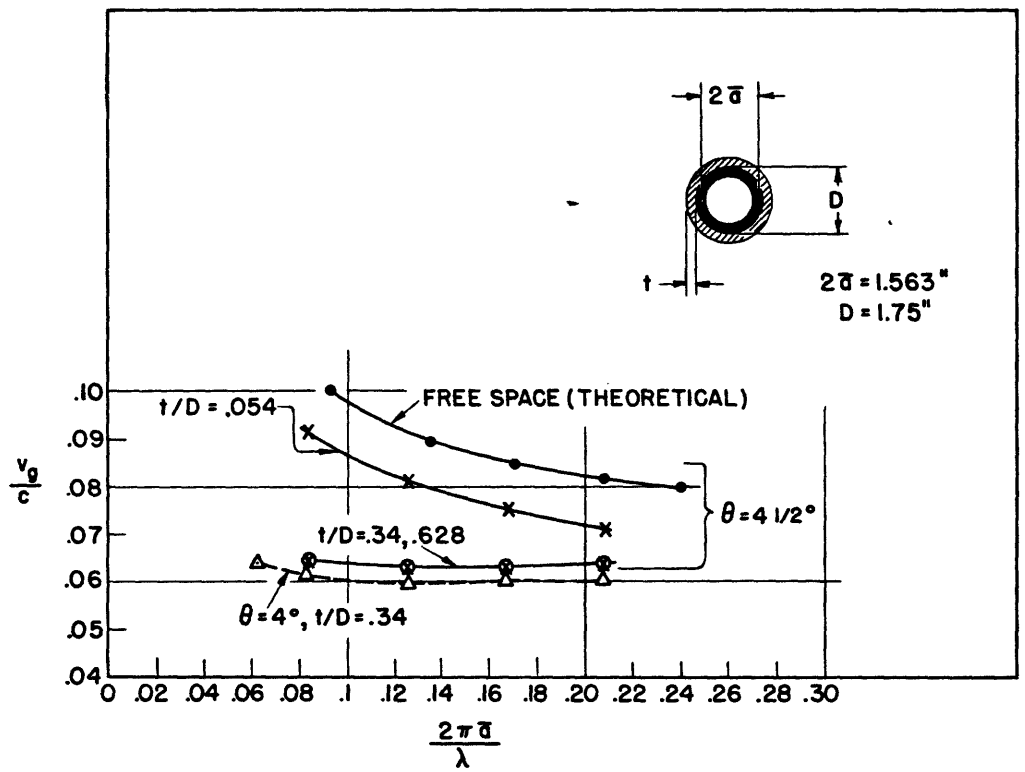

Fig.7 Measured phase-velocity characteristics of a charge-free helix supported by dielectric shells of various thicknesses.

The computation of the guiding properties of a helix enclosed in a dielectric shell of finite thickness is a very tedious task. The relatively thick glass tubes used in practice, and the rapid radial attentuation of the wave, however, enable us to consider the wall as infinitely thick. Solution of the boundary-value problem for the case of a thin helical sheath in an infinitely thick dielectric shell yields the following expression:

$$\frac{p_2}{p_1}\left\{\frac{1-\dfrac{k_2^2\, I_1^2(p_2a)}{p_2^2\, I_o^2(p_2a)}\cot^2\theta}{\dfrac{I_1(p_2a)}{I_o(p_2a)}}\right\}$$

$$= -\frac{K_o(p_1a)}{K_1(p_1a)} + \frac{k_1^2}{p_1^2}\cot^2\theta\,\frac{K_1(p_1a)}{K_o(p_1a)}\ ;$$

where

a = helix radius,

ϵ_1 = permittivity outside the helix,

ϵ_2 = permittivity inside the helix,

$k_1^2 = \omega^2\epsilon_1\mu$,

$k_2^2 = \omega^2\epsilon_2\mu$,

γ = propagation constant along the helix,

$p_1^2 = -(k_1^2 + \gamma^2)$

$p_2^2 = -(k_2^2 + \gamma^2)$

θ = pitch angle of the helix,

$I_\nu(x)$ and $K_\nu(x)$ are the modified Bessel functions defined by

$$I_\nu(x) = j^{-\nu} J_\nu(jx)$$

$$K_\nu(x) = \frac{\pi}{2} j^{\nu+1} H_\nu^{(1)}(jx).$$

Figure 8 shows the phase velocity computed from the above expression with $\epsilon_2 = \epsilon_0$ (free space), $\frac{\epsilon_1}{\epsilon_2} = 4.5$, and $\theta = 4^\circ$ and 5°.

We observe in both Figures 7 and 8 that the phase velocity is considerably less than for the helix in free space, and there is much less dispersion. The differences between experiment and theory (Figures 7 and 8) are probably due to the finite wire thickness, which has the effect of partially shielding the dielectric from the field between the wires. A further confirmation of this hypothesis may be found in a comparison of the two curves in Figure 7. The actual variation of velocity with the pitch angle is not

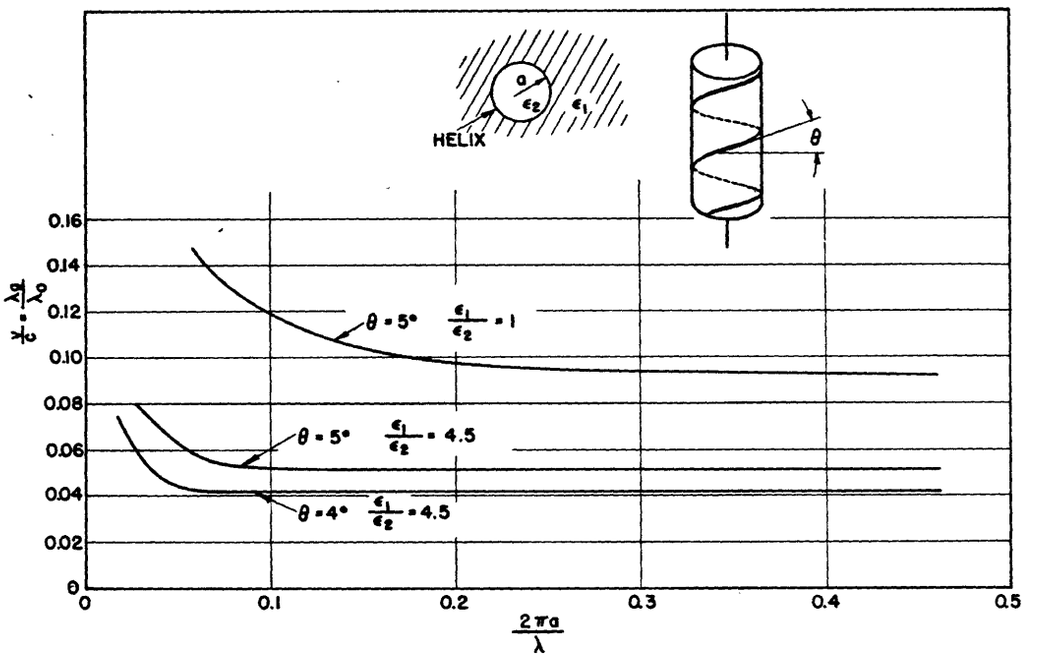

Fig.8 Computed phase-velocity characteristics of a charge-free helix surrounded by an infinite dielectric.

so great as the theory would lead us to expect (Figure 8). Since the wire diameter was the same for the two curves of Figure 7, the effective shielding was greater in the case of the smaller pitch.

Conclusions

On the basis of the experiments described above, it is possible to establish certain electrical criteria which should be satisfied by the mechanical construction of the tube:

1. Insofar as possible, the helix diameter should be proportioned to make the gain a maximum within the pass band. For velocities of about 0.1 c, the ratio $\frac{2\pi a}{\lambda}$ should be about 0.1.

2. The dielectric supporting structure should be arranged so as to maintain the dispersive character of the helix. This will reduce the electronic gain at frequencies outside the pass band of the tube and thereby decrease the tendency toward oscillation.

3. The use of a support with lower dielectric constant than that of glass or quartz would make the actual helix approximate an ideal helix. A promising approach to this end has been made by the use of tubular supports made of glass wool, sintered to form a rigid structure. These have been made with an effective dielectric

constant of about 1.3. The tubes are made in one-inch lengths by packing the wool into a steel cylinder with an inner core to give the appropriate inner and outer diameters. The sintering is done in a furnace at about 700°C. At present, a tube with these supports has not yet been made; but we hope to be able to report on such a tube soon.

Appendix I.

Analysis of Standing-Wave Patterns

Assume two propagation constants γ_1 and γ_2. There will then be two incident and two reflected waves. The electric field will contain the following components:

$$\begin{aligned} &A_1 \cos(\omega t - \gamma_1 x) \ , \\ &\Gamma_1 \cos(\omega t + \gamma_1 x) \ , \qquad \gamma_1 = 2\pi/\lambda_1 \\ &A_2 \cos(\omega t - \gamma_2 x) \ , \\ &\Gamma_2 \cos(\omega t + \gamma_2 x) \ , \qquad \gamma_2 = 2\pi/\lambda_2 \end{aligned}$$

where $\gamma_1 \approx (1/10)\gamma_2$. The instantaneous electric field at a point on the line is given by the sum of the fields above. The detector indicates the time average of the square of the sum, represented by the following expression:

$$A_1\Gamma_1 \cos 2\gamma_1 x + A_2\Gamma_2 \cos 2\gamma_2 x + (A_1 A_2 + \Gamma_1 \Gamma_2)\cos(\gamma_1 - \gamma_2)x$$

$$(A_1\Gamma_2 + A_2\Gamma_1)\cos(\gamma_1 + \gamma_2)x \ ,$$

plus a constant term. These four waves have wavelengths $\lambda_1/2$, $\lambda_2/2$, $\lambda_1\lambda_2/(\lambda_1+\lambda_2)$ and $\lambda_1\lambda_2/(\lambda_2-\lambda_1)$. Since $\lambda_2 \approx 10\lambda_1$, the two composite waves will have wavelengths about equal to λ_1 ($\pm 10\%$).

Measurement of the various periods observable in Figure 3 gives the following results:

	$\lambda_2/2$	λ_1^*	$\lambda_1/2$
Measured	.52λ	.102λ	.051λ
Theoretical	.50λ	.105λ	.052λ

* λ_1 is the average of a number of periods corresponding to a mixture of $\lambda_1\lambda_2/(\lambda_1+\lambda_2)$ and $\lambda_1\lambda_2/(\lambda_1-\lambda_2)$.

Appendix II.

Measurements of Helix Phase-Velocity Characteristics

The measurements of phase velocity described in this report were made by observing the distance between nodes of the standing wave on the helix. The complicated character of the curve in Figure 3 indicates the importance of exciting only the desired node.

Initially, the measurements were made with a probe moving outside the helix and connected to a sensitive receiver. The use of thicker dielectric shells reduced the sensitivity of this arrangement below the useful level. To overcome this difficulty, a dielectric rod with a metal plate on the end was pushed into the load end of the helix. A crystal detector and meter were placed in parallel with the input to the helix. As the rod was pushed into the helix, the crystal current varied periodically. By noting the motion of the rod corresponding to the distance between two minima of the crystal current, the wavelength could be determined. Both of these methods gave identical results when used for the same measurements.

References

1. R. Kompfner, Proc. I.R.E. 35, 124 (1947).
2. J. R. Pierce, Proc. I.R.E. 35, 111 (1947).
3. L. J. Chu and D. Jackson, "Field Theory of Traveling-Wave Tubes" R.L.E. Report No. 38, April 28, 1947; also Proc. I.R.E. 36, 853 (1948)
4. O. E. H. Rydbeck, Ericsson Technics No. 46 (1948).
5. C. Shulman and M. S. Heagy, RCA Review Vol. VIII, No. 4 (1947).
6. C. C. Cutler, Proc. I.R.E. 36, 230 (1948).